SSRG International Journal of Applied Physics
ISSN: 2350-0301/ https://doi.org/10.14445/23500301/IJAP-V9I3P101

Volume 9 Issue 3, 1-18, Sep-Dec 2022

Original Article

The Effect of Atmospheric Transmittance of UVB Solar Irradiance to Broadband Solar Radiation at Different Climate Sites

Samy A. Khalil

Solar and Space Department, National Research Institute of Astronomy and Geophysics (NRIAG), 11421, Helwan, Cairo, Egypt.

Received: 22 August 2022 Revised: 02 October 2022 Accepted: 15 October 2022 Published: 28 October 2022

Abstract *- In the present research, the continuous measurements of global solar radiation (G) and UVB solar radiation are taken in different climate sites during the period time from 1986 to 2020 for all weather conditions. The differences between measured and calculated UVB solar energy values vary from 1% to 2.2%. The average hourly UVB radiation intensity ratio to the current study's total global solar radiation was 0.294%. In contrast, the ratio of $UVB_{ext.}$ to the corresponding $G_{ext.}$, $UVB_{ext.}/G_{ext.}$, was 1.563%, demonstrating the much greater degree of attenuation of UVB relative to global solar radiation. The UVB transmission through the climate can be evaluated during the current investigation, where the typical hourly estimations of UVB transmission are declining due to the air as a daytime component. The change in the monthly average of hourly UVB/G% may be caused by the increase and decrease of both G and UVB's monthly average hourly values. The monthly average mean UVB/G varies from 0.15% in January to 0.30% in June. The average hourly UVB/G% was also lower in the afternoon compared to the morning. The effect of aerosols on the fluctuation in air transparency may have contributed to the lower UVB/G% levels in the afternoon. The average values of UVB solar energy reduction throughout this research were 92.21%, 90%, 90.2%, and 90.1 for Hurghada, El-Kharga, Dammam, and Hail, respectively, in the present study. Inversely, the relationship between UVI levels and solar zenith angle (SZA) at all selected locations. The monthly mean values of RAF under clear skies were equal to 1.058, 1.003, 1.027, and 1.087 for Hurghada, El-Kharga, Dammam, and Hail sites in the present research. The monthly mean values under clear skies, UVB values rise by 1.058%, 1.003%, 1.027%, and 1.087% if the slant ozone value at all examined sites decreases by 1%. Ozone variations at high angles result in non-linear UVB transmission.*

Keywords *- Atmospheric transmittance, Solar energy, Solar zenith angle, UVB solar energy.*

1. Introduction

Visible and near-infrared wavelengths dominate extraterrestrial solar radiation, and only a small portion of the energy is within the UV region. Then, only a fraction of this UV radiation incident at the top of the atmosphere is transmitted to the Earth's surface. This spectrum of solar radiation directly affects human health, terrestrial and aquatic ecosystems, and the degradation of materials [1, 2]. The range of electromagnetic energy emitted by the sun is known as the solar spectrum and lies mainly in three regions: ultraviolet (UV), visible, and infrared (IR). A part of this radiation reaches the Earth's surface by passing through the atmosphere. This part's intensity is controlled by various factors, such as astronomical factors and atmospheric compounds. The astronomical factors are the Earth-Sun distance and the solar zenith angle (SZA). Solar radiation is weakened during its transit through the atmosphere by several processes. These processes include absorption (by several gases) and scattering (by molecules, clouds, and aerosols). The absorption of solar radiation in the atmosphere is due mainly to ozone in the UV range and water vapour in specific bands in the IR range of the solar spectrum. Besides ozone and water vapour, the main gaseous absorbers are CO_2 and O_2 [3-5].

Solar radiation received by Earth is vital for the Earth–atmosphere system energy balance. Renewable solar energy and climate models verification and a good understanding of solar irradiance and its short-term and long-term trends are essential for many applications. UV radiation forms a small fraction of the solar spectrum with wavelengths 100–400 nm, making about 8.73% of the spectrum at Earth's surface [6]. UV radiation is commonly categorized into three different wavelength bands depending on harmful results on the skin: UVC (100–280 nm), which is completely depleted by ozone and oxygen; UVB (280–320 nm), which is consumed by ozone, and UVA (320–400 nm), which is slightly affected by ozone. UVC, UVB, and UVA represent 1.5%, 1.33%, and 5.9% of the solar spectrum, respectively.

On the one hand, a little to moderate dose of ultraviolet solar radiation is fundamental in producing vitamin D3. Conversely, extra amounts can harm the skin and eyes [7]. UV radiation changes greatly with latitude and local time due to the change in the sun's elevation. In addition, UV radiation is usually affected by environmental conditions. UVB is responsible for sunburns and suppression of the human immune system. Due to its double-edged sword impact, UVB radiation has recently attracted substantial attention. Many researchers have discussed the advantage and disadvantages of UVB radiation. UV-B radiation received at the Earth's surface is highly variable. It shows a strong dependence on solar zenith angle (SZA) and ozone amount, leading to large geographical and temporal variability [8-10].

UVB accounts for 80% of the destructive effects of sun exposure despite being only a small fraction of extraterrestrial solar radiation. Several authors have studied and reported UVB's beneficial and damaging effects on humans, ecosystems, animals, plants, and materials [10-13]. UVB represents only a small part of the spectrum at the Earth's surface. The literature noted that, for different locations, the radiometric ratio UVB/G varies from 0.02 to 0.8% [14-16]. The changes in UVB/G are due to variations in certain geometric factors and atmospheric compounds. The atmospheric compounds strongly influencing UVB are ozone, aerosols, and clouds. In addition, other gases control radiation levels in the G range at the Earth's surface, for example, water vapour by [17-20].

The measured UV at constant periods to investigate daily, monthly, and yearly radiation in Riyadh, Kingdom of Saudi Arabia by [21]. The author concluded that different climate factors significantly impact Riyadh's UV scattering, UV reflection, ozone, and cloud layers. UVB/G ratio variations are related to the change in different geophysical parameters. Published data indicate a broad UVB/G ratio change (0.02–0.80%) for sites [22]. A UVB/G ratio variation is attributed to the strong spectral dependence of solar radiation transmittance on optical air mass, which results in various changes in incident solar UVB and G. The examined UVB/G ratio under several atmospheric conditions at Athalassa, Cyprus by [23]. They reported an average of 3.5% for Cairo, Egypt, while Valencia, Spain, recorded a monthly average of 2.7% to 5.2% [24]. Lee et al. examined the spectral dependence of aerosols, ozone, and clouds on UVB, UV, and G in South Korea [25-27]. They showed that the UVB/G ratios increased with decreasing clearness index, indicating that UVB and G were affected differently by various attenuating parameters.

The impact of aerosols and clouds on G and UVB was studied using measurements from various South Korean locations [28]. They concluded that the ratio (UVB/G) was inversely proportional to K_t, which indicated that UVB and G were influenced differently by different attenuating parameters. The authors also investigated the relationship between K_t and the clearness index of UVB radiation (K_{tUVB}) for each site in their study. They illustrated that the relation between the two parameters was not exactly linear because of the various impacts of weather conditions on G and UVB. (UVB/G) increases with cloud cover, showing that G penetrated clouds more effectively than UVB. They stated that the clouds and aerosol's impacts on G and UVB were related to local climate variations [29].

Monitoring of mean UV radiation from 2003 to 2017 at various locations in Saudi Arabia is carried out by [30] to determine UVB, UVBext, UVI, $K_{TUVB,}$ and total ozone column. The calculated UVB agrees well with UVB measurements. The recorded and estimated UVB radiation error varies from 1.27 to 3.87%.

The main objective of this research, we used the hourly and monthly data on UVB solar radiation collected during the period time from 1986 to 2020 at different climatic change sites in Egypt and Saudi Arabia countries to evaluate the significantly reduces (UVB/G) at the surface of the Earth in comparison to its magnitude at the atmospheric top. The reduction is substantial because of atmospheric parameters that attenuate UVB more efficiently than G. The variation in the hourly ratio (UVB/G) as a function of $K_{T,}$ as well as the relationship between global clearness index (K_T) and UVB clearness index (K_{TUVB}), are studied.

2. Materials and Methods Analysis

In this study, we used the hourly and monthly data on UVB solar radiation collected during the period time from 1986 to 2020 at different climatic change sites in Egypt and Saudi Arabia countries. The Egyptian Metrological Authority (EMA) is responsible for the scientific advice and calibration of the Egyptian Monitoring Network. Hourly values (hour integral irradiance in MJ m^{-2} h^{-1}) of UVB and global solar radiation (G) at the horizontal surface. The Model UVB−1 Ultraviolet broadband radiometer No. 960842, Yankee Environmental Systems, Inc. (YES), has been used to measure the total irradiance from 280 to 320 nm. In addition, the Precision Spectral Pyranometer (PSP) No. 16317IS (an ISO 9060 secondary standard Pyranometer spectral range (295–2 800 nm) used for the precise measurement of global solar radiation. The PSP is the most common Pyranometer used by National Meteorological Authorities in worldwide meteorological networks. The Combilog Datalogger (No. 1020, TH. Friedrichs & CO., Germany) recorded the values used to estimate spatially distributed daily values of total ozone column amount expressed in Dobson Units (DU) by [22-24]. Used TOM's data to study the relationship between atmospheric ozone and erythemal ultraviolet irradiance (UVER) between 280 and 400 nm [15]. In addition, concluded that the TOMS global ozone is about only 1% higher than the ground

measurements in 30 mid-northern latitude stations [19]. Furthermore, a good agreement between satellite and ground-based ozone data. TOMS (Earth Probe: 1996–2005) passes over Hurghada approximately between 10:00 and 12:00 UTC; thus, the used ground data of UVB represents an average for values recorded in the mentioned interval by [15-17]. Similarly, solar zenith angles were average for the mentioned interval. As a result, this study deals with 6155 simultaneous data of UVB, G, and total ozone column (TOC) through the period from 1986 to 2020. The values of UVB and those of single daily (TOMS) ozone could be the representative value for the whole 2–h period. All data used in this work are obtained as a daily average between 10:00 and 12:00 UTC. The data in Saudi Arabia were obtained from the Meteorological and Environmental Protection Agency (MEPA) Saudi Arabia. Ultraviolet irradiation is measured using an Eppley radiometer TUVR No. 31737. Its sensitivity and cosine response are approx. 150 μV/(W/m^2) and ± 3.5% from normalization 0-70^o zenith angle. In addition, total ozone column data (TOC, DU) were obtained from the Total Ozone Mapping Spectrometer **(**TOMS) satellite (http:juic. gsfc.NASA.Gov/ index.html) which was given around 12:00 GMT. These instruments are calibrated yearly against a reference instrument traceable to the World Radiometric Reference (WRR) maintained at Davos, Switzerland (WRC, 1985, 1995). The absolute accuracy of calibration is ±3–4%. The resolution of these instruments is 1 W m^2. The hourly values of hemispherical transmittances for UVB and *G* (K_{tUVB} and K_t, respectively) were also calculated [28, 29]. The information on the selected sites in the present study is summarized in table (1).

Table 1. Information on the selected locations in the present study

Locations	Country	Lat. (°N)	Long. (°E)	Elevation(m)	The period of data	Error percentage
El-Kharga	**Egypt**	25^0 45'	30^0 55'	32 m	1986-2020	4.7
Hurghada		27^0 15’	33^0 48’	14 m	1986-2020	5.2
Dammam	**Saudi Arabia**	26^0 23’	49^0 53’	10 m	1986-2020	6.5
Hail		27^0 52'	41^0 69'	992 m	1986-2020	3.9

3. The Collected Data

In the present research, we used the average hourly and monthly mean of data on UV solar radiation collected during the period time from 1986 to 2020 at four-area different climate zones located in Egypt (Hurghada and El-Kharga) sites and Saudi Arabia (Dammam and Hail) locations. The proposed present research is to evaluate the hourly and monthly average of the ultraviolet (UV) solar radiation component (UVBext, UVB, UVI, and clearness index UV) and total ozone column (TOC). The data were obtained from the Meteorological and Environmental Protection Agency (MEPA) in Saudi Arabia, while obtaining the data for the selected locations in Egypt was from the Egyptian Meteorological Authority (EMA).

The monthly average of the main statistics (Minimum, Maximum, Range, Mean, Median, Standard error, Average deviation, and Standard deviation) of UVB, UVBest., $K_{tUVB,}$ and TOC (MJ.m^{-2}h^{-1}) at the selected locations in the present research during the period time from 1986 to 2020 are shown in tables (2&3). These tables indicate that the mean and median values for all locations in the present research are nearest to them. It is due to the quality of data used in this paper. In addition to the standard deviation values, the average deviation and standard error are very small. The accuracy of the present research data does not exist at 7%.

The data frequency histogram of the selected locations in the present research (Hurghada, El-Kharga, Dammam, and Hail) during the period time from 1986 to 2020 is clearly in figure 1. The high variability of the monthly values of both UVB radiations during the period time in this research is demonstrated by cumulative frequencies of monthly total UVB radiation.

Table 2. The main statistics of UVB, UVBest., $K_{tUVB,}$ and TOC (MJ.m^{-2}h^{-1}) at Hurghada and El-Kharga sites

Hurghada	UVB	UVBest.	K_{tUVB}	TOC	El-Kharga	UVB	UVBest.	K_{tUVB}	TOC
Number of values	420	420	420	420		420	420	420	420
Minimum	0.0032	0.0029	0.0119	283.4		0.0034	0.0032	0.0115	272.8
Maximum	0.0131	0.0127	0.125	338.7		0.0133	0.0130	0.122	348.6
Range	0.0092	0.0096	0.057	77.5		0.0095	0.0099	0.1117	68.2
Mean	0.0084	0.0083	0.094	302.7		0.0079	0.0086	0.0951	309.8
Median	0.0083	0.0082	0.093	293.4		0.0078	0.0085	0.0953	311.5
Standard error	0.0003	0.0003	0.0011	1.269		0.0002	0.0002	0.0013	1.124
Average deviation	0.0023	0.0023	0.0132	13.98		0.0024	0.0024	0.0141	12.86
Standard deviation	0.0027	0.0027	0.0155	16.94		0.0029	0.0029	0.0174	14.86

Table 3. The main statistics of UVB, UVBest., K_{tUVB}, and TOC ($MJ.m^{-2}h^{-1}$) at Dammam and Hail locations

Dammam	UVB	UVBest.	K_{tUVB}	TOC	Hail	UVB	UVBest.	K_{tUVB}	TOC
Number of values	420	420	420	420		420	420	420	420
Minimum	0.0031	0.0033	0.0113	274.35		0.0029	0.0028	0.057	234.8
Maximum	0.0128	0.0133	0.1225	338.7		0.0126	0.0128	0.1224	342.8
Range	0.0102	0.0104	0.1107	55.86		0.0096	0.0099	0.0634	112.5
Mean	0.0078	0.00781	0.0920	308.6		0.0076	0.0078	0.0925	304.8
Median	0.0077	0.0082	0.0922	306.4		0.0077	0.0079	0.0927	303.2
Standard error	0.0004	0.0004	0.0012	0.9896		0.0003	0.0003	0.0125	1.113
Average deviation	0.0022	0.0022	0.0137	11.4		0.0024	0.0024	0.0144	11.89
Standard deviation	0.0026	0.0026	0.0173	11.96		0.0027	0.0027	0.0168	15.32

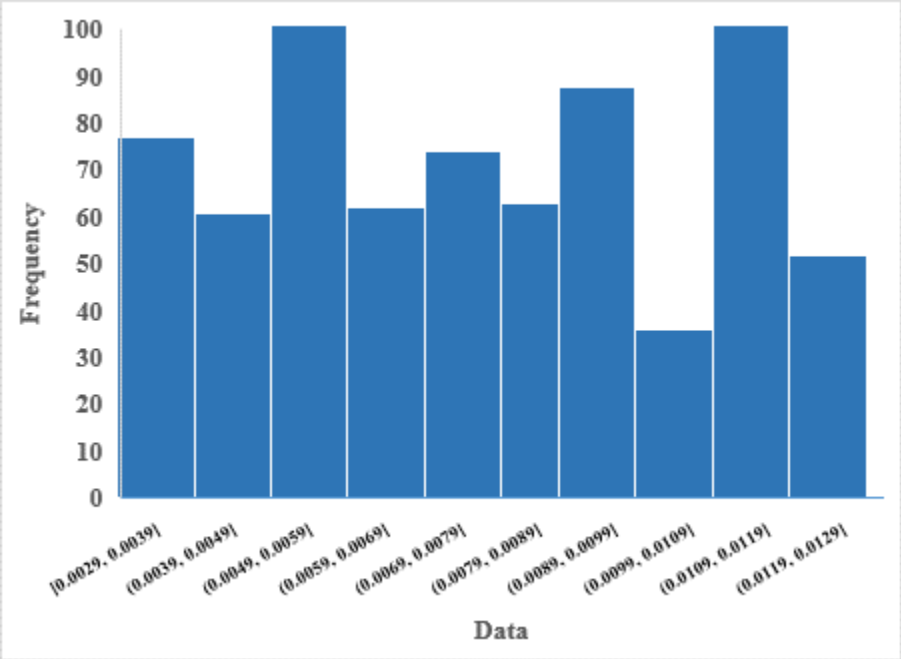

Fig. 1 The data frequency histogram from 1986 to 2020 for selected sites in the present research ($MJ/m^2/h$)

4. Theory of Methodology

The UVB hemispherical transmittance is defined as follows [16-21].

$$K_{TUV} = \frac{UVB}{UVBext.} \quad (1)$$

Where UVB_{ext}, is the extraterrestrial solar radiation value on a horizontal surface, it is given by:

$$UVB_{ext.} = I_{SCUVB}\,(12/\pi)\,E_0 \int_{\omega 2}^{\omega 1} sin\ sin\ (\Theta) d\omega \quad (2)$$

Where (Θ) is the solar elevation angle, E_0 is the correction factor for the eccentricity of the Earth's orbit, w_i (i=1and 2) is the solar our angle at the beginning of the period and the end of the period, respectively, and I_{SCUVB} is the UVB solar constant (21.51 Wm^{-2}). It has been obtained from the spectral values [16-21].

The extraterrestrial solar radiation on a horizontal surface is calculated from the following Equation [4, 22-25].

$$G_{ext} = (24x3.6 \times 10^{-3} \times I_{sc})/\pi\ [1+ 0.033 \cos (360\tfrac{D}{365})]\ \cos\phi \cos\delta \sin\omega + \omega \sin\phi \sin\delta \quad (3)$$

Where D is the Julian day number, I_{sc} = 1367 Wm^{-2} is the solar constant, ϕ is the latitude of the location, **δ** is the declination angle given as:

$$\delta = 23.45 \sin (360\tfrac{248+D}{365}) \quad (4)$$

Moreover, **ω** is the sunset hour angle given as:

$$\omega = \cos^{-1} (-\tan\phi \tan\delta) \quad (5)$$

The hourly value of hemispherical transmittance (K_t) is defined as the ratio of the global solar radiation on a horizontal surface at the ground (G) to the outside of the Earth's atmosphere ($G_{ext.}$) [4, 26].

$$K_t = G/G_{ext} \quad (6)$$

Where (a) and (b) are regression coefficients that depend on the weather parameters of the selected location.

The measurements of UVB were converted into UVER (solar ultraviolet erythematic irradiance) values employing conversion factors (Diffey factor) provided by [74-76], and from them, UVI (ultraviolet indices) hourly values were evaluated [4, 24-26]. The values of UVI radiation have also been obtained from spectral calculated weighted by the erythema radiation action spectrum; they are represented by (UVI) model and can be obtained by the following expression:

$$(UVI)_{model} = K_{er} \int_{290}^{400} E_\lambda S_{er}(\lambda) d\lambda \quad (7)$$

Where K_{er} is 40 m^2W^{-1}, $E_\lambda$is the UV spectrum wavelength dependent ($Wm^{-2}nm^{-1}$) and S_{er} is the erythemal weighting function accepted by CIE (Commission International d'Eclairage).

The slant total ozone column (TOC), Dobson (DU), represents the actual ozone amount in the atmosphere as follows [4, 15-18].

$$Z = TOC/(SZA) \quad (8)$$

Where (SZA) is the cosine of the solar zenith angle; this expression is only valid for direct solar irradiance).

The relation between the UV index and solar zenith angle (SZA) is as follows Equation [27, 28].

$$UVI = a\,(SZA)^b \quad (9)$$

Where (a) and (b) were determined from the least squares fitting.

The slant ozone column proposes a natural expansion of the Radiation Amplification Factor (RAF) for UVER to consider all solar zenith angle cases together. RAF is a useful indicator of the sensitivity of UVER to ozone changes. High RAF values indicate that the UVER values are strongly sensitive to changes in stratospheric ozone, while small RAF values indicate that UVER is less sensitive to ozone changes [24]. In this direction, they analyzed the relationship between measurements of UVER recorded at Badajoz, Spain, and the total ozone column estimated by the instrument TOMS/NASA.

The new RAF parameter is formulated by power equation using slant ozone (*Z*) and UVER atmospheric transmission (K_{tUVER}) values as follows [24, 25, 27].

$$K_{tUVER} = CZ^{-RAF} \quad (10)$$

Where *C* is related to other atmospheric constituents that also scatter and absorb UVER, such as cloudiness, aerosols, and tropospheric ozone.

In analogue with the UVER case, it is possible to use *Z* to quantify the relationship between UVB transmission (K_{tUVB}) and the total ozone column. Thus, Equation (11) can be written as follows:

$$K_{tUVB} = CZ^{-RAF} \quad (11)$$

In addition, the determination of the Radiation Amplification Factor for UVB (RAF) can be estimated. RAF is considered one of the frequently used means to express the impact of ozone depletion on UVB values. RAF is defined as the percentage increase in UVB resulting from a 1% decrease in the column amount of atmospheric ozone [24, 89]. Thus, it was proposed to study the relationship between atmospheric ozone and UVB. In addition, it has been used widely as a useful parameter during the last few years [21, 27].

5. Results and Discussion

Tables (4–7) present, for the sites of Hurghada, El-Kharga, Dammam, and Hail, respectively, the monthly and seasonal averages of extraterrestrial UVB solar radiation, measured and estimated UVB solar radiation, clearness index K_{tUVB} of UVB radiation, C_V, K_{tUVB}, and TOC (DU). These tables show that the maximum values of the above parameters occur during the summer, while the minimum values occur during the winter. However, it is evident from some variables' values that they fluctuate between summer and winter levels in the spring and autumn. The mean UVB solar radiation values for all chosen locations range from 0.0044 to 0.0129 MJ m-2 h-1, while the UVB_{est}. Values range from 0.0046 to 0.0124 for all locations in the current study.

Furthermore, it is evident from the tables that the calculated values of UVB solar energy levels and the measured UVB solar radiation values coincide well. The discrepancy between measured and calculated UVB solar energy values ranges from 1% to 2.2%. The worldwide radiation k_t values for the average monthly UVB clearness index (K_{tUVB}) are lower. The value of the global solar radiation (G) is divided by the value of the extraterrestrial global solar radiation ($G_{ext.}$), where k_t is the value. However, for all locations in the current investigation, the K_{tUVB} values range from 0.084 to 0.119. The exceptionally strong

attenuation of UVB light by stratospheric ozone and scattering processes is the cause of this behavior. These data also show that for all of the areas chosen for the current research, C_v values are lowest around the summer months and highest throughout the winter months.

Cv levels between the highest and lowest values are also found in the spring and autumn months. The relatively high stability of the local climate during this period, i.e., the fact that there is very little variation in climatic conditions from one month to the next, is what led to the finding that the lowest coefficient of variation characterizes the months. The sun's apparent daily motion around the Earth causes UVB_{ext}. Solar radiation behaves the way it does. The study of UVB solar energy behavior at the Earth's surface reflects the influence of the atmosphere on that radiation.

Additionally, we see from these tables that for all of the places chosen for the current research, the values of the total ozone column (DU) are maximum around the spring months. In contrast, the values of TOC in the summer, autumn, and winter seasons are closest to them. The exceptionally strong attenuation of UVB light by stratospheric ozone and scattering processes is then the cause of this phenomenon. The fact that ratio of the average hourly UVB radiation intensities to the total global solar radiation in the current study from 1968 to 2020 was 0.294%, whereas the ratio of $UVB_{ext.}$ to the corresponding $G_{ext.}$, $UVB_{ext.}/G_{ext.}$, was 1.563%, demonstrates the much greater degree of attenuation of UVB relative to global solar radiation. The comparison between the observed and calculated data of UVB solar energy during the period time from 1968 to 2020 for all selected locations in the present research is shown in figure 2. Good agreements of measured and calculated values of UVB were obtained.

Table 4. Monthly and seasonal averages of UVB_{ext}. UVB, $UVB_{est.}$, C_V, $K_{tUVB,}$ and TOC (DU) at the Hurghada location during the period time from 1986 to 2020 in the present research.

Month	UVBext. ($MJ\ m^{-2}\ h^{-1}$)	UVB ($MJ\ m^{-2}\ h^{-1}$)		UVBest. ($MJ\ m^{-2}\ h^{-1}$)		C_V %	KtUVB	TOC (DU)	
		Mean	SD	Mean	SD			Mean	SD
Jan.	0.0521	0.0046	0.0008	0.0051	0.0009	47	0.088	263	15
Feb.	0.0652	0.0063	0.0019	0.0064	0.0013	51	0.096	271	16
Mar.	0.0769	0.0084	0.0022	0.0091	0.0016	43	0.109	288	13
Apr.	0.0875	0.0099	0.0017	0.0099	0.0015	45	0.113	309	17
May	0.0968	0.0115	0.0013	0.0111	0.0017	41	0.119	302	12
Jun.	0.1034	0.0118	0.0011	0.0123	0.0014	38	0.114	289	14
Jul.	0.1018	0.0113	0.0015	0.0115	0.0018	34	0.111	291	9
Aug.	0.0942	0.0101	0.0012	0.0108	0.0011	31	0.107	275	8
Spt.	0.0868	0.0091	0.0018	0.0095	0.0015	42	0.104	281	6
Oct.	0.0753	0.0077	0.0021	0.0072	0.0019	46	0.102	269	11
Nov.	0.0648	0.0062	0.0024	0.0058	0.0016	52	0.096	279	13
Dec.	0.0537	0.0049	0.0022	0.0047	0.0014	56	0.091	259	12
Winter	0.0571	0.0053	0.0015	0.0054	0.0012	51	0.092	264	14
Spring	0.0871	0.0082	0.0021	0.0085	0.0016	43	0.094	300	11
Summer	0.0998	0.0111	0.0024	0.0116	0.0019	34	0.111	285	7
Autumn	0.0756	0.0077	0.0017	0.0075	0.0015	47	0.102	276	9

Table 5. Monthly and seasonal averages of UVB_{ext}. UVB, $UVB_{est.}$, C_V, $K_{tUVB,}$ and TOC (DU) at the El-Kharga location during the period time from 1986 to 2020 in the present research.

Month	$UVB_{ext.}$ ($MJ\ m^{-2}\ h^{-1}$)	UVB ($MJ\ m^{-2}\ h^{-1}$)		$UVB_{est.}$ ($MJ\ m^{-2}\ h^{-1}$)		C_V %	K_{tUVB}	TOC (DU)	
		Mean	SD	Mean	SD			Mean	SD
Jan.	0.0523	0.0044	0.0011	0.0048	0.0008	45	0.084	259	13
Feb.	0.0648	0.0061	0.0017	0.0057	0.0015	53	0.094	267	15
Mar.	0.0763	0.0082	0.0021	0.0088	0.0013	46	0.105	282	11
Apr.	0.0872	0.0096	0.0015	0.0092	0.0012	47	0.110	311	14
May	0.0964	0.0113	0.0012	0.0116	0.0015	44	0.117	308	18
Jun.	0.1031	0.0116	0.0014	0.0119	0.0012	36	0.113	294	13
Jul.	0.1015	0.0111	0.0012	0.0113	0.0014	32	0.109	286	8
Aug.	0.0937	0.0102	0.0015	0.0105	0.0011	35	0.108	272	6

Spt.	0.0862	0.0093	0.0016	0.0096	0.0013	46	0.107	267	9
Oct.	0.0751	0.0079	0.0023	0.0075	0.0016	49	0.105	262	13
Nov.	0.0645	0.0064	0.0021	0.0061	0.0012	54	0.099	285	15
Dec.	0.0534	0.0047	0.0018	0.0051	0.0011	53	0.088	264	10
Winter	0.0568	0.0051	0.0015	0.0052	0.0011	50	0.090	263	13
Spring	0.0866	0.0097	0.0016	0.0099	0.0013	47	0.112	300	14
Summer	0.0994	0.0110	0.0014	0.0112	0.0012	34	0.110	284	8
Autumn	0.0753	0.0079	0.0020	0.0077	0.0013	49	0.105	271	12

Table 6. Monthly and seasonal averages of $UVB_{ext.}$ UVB, $UVB_{est.}$, C_V, $K_{tUVB,}$ and TOC (DU) at the Dammam location during the period time from 1986 to 2020 in the present research.

Month	$UVB_{ext.}$ ($MJ\ m^{-2}\ h^{-1}$)	UVB ($MJ\ m^{-2}\ h^{-1}$)		$UVB_{est.}$ ($MJ\ m^{-2}\ h^{-1}$)		C_V %	K_{tUVB}	TOC (DU)	
		Mean	SD	Mean	SD			Mean	SD
Jan.	0.0525	0.0048	0.0014	0.0046	0.0011	47	0.091	263	16
Feb.	0.0646	0.0067	0.0019	0.0055	0.0016	55	0.104	274	14
Mar.	0.0767	0.0085	0.0023	0.0082	0.0017	43	0.111	289	12
Apr.	0.0875	0.0091	0.0018	0.0097	0.0015	44	0.104	318	13
May	0.0968	0.0118	0.0015	0.0114	0.0018	48	0.122	306	12
Jun.	0.1033	0.0123	0.0014	0.0117	0.0011	39	0.119	297	9
Jul.	0.1018	0.0116	0.0013	0.0115	0.0013	35	0.114	281	10
Aug.	0.0934	0.0108	0.0011	0.0109	0.0014	34	0.116	275	8
Spt.	0.0865	0.0098	0.0012	0.0095	0.0016	42	0.113	269	7
Oct.	0.0753	0.0083	0.0018	0.0079	0.0019	48	0.110	256	11
Nov.	0.0642	0.0069	0.0016	0.0064	0.0015	51	0.107	277	16
Dec.	0.0531	0.0054	0.0014	0.0052	0.0013	48	0.102	269	12
Winter	0.0567	0.0056	0.0016	0.0051	0.0013	50	0.099	269	14
Spring	0.0870	0.0098	0.0019	0.0097	0.0017	45	0.113	304	12
Summer	0.0995	0.0116	0.0013	0.0114	0.0013	36	0.117	284	9
Autumn	0.0753	0.0083	0.0015	0.0079	0.0015	47	0.110	267	11

Table 7. Monthly and seasonal averages of $UVB_{ext.}$ UVB, $UVB_{est.}$, C_V, $K_{tUVB,}$ and TOC (DU) at Hail location during the period time from 1986 to 2020 in the present research.

Month	$UVB_{ext.}$ ($MJ\ m^{-2}\ h^{-1}$)	UVB ($MJ\ m^{-2}\ h^{-1}$)		$UVB_{est.}$ ($MJ\ m^{-2}\ h^{-1}$)		C_V %	K_{tUVB}	TOC (DU)	
		Mean	SD	Mean	SD			Mean	SD
Jan.	0.0529	0.0051	0.0012	0.0049	0.0013	49	0.094	258	13
Feb.	0.0651	0.0072	0.0017	0.0065	0.0019	51	0.111	271	12
Mar.	0.0771	0.0081	0.0021	0.0086	0.0015	45	0.105	284	11
Apr.	0.0872	0.0095	0.0015	0.0091	0.0012	46	0.109	315	14
May	0.0964	0.0124	0.0012	0.0119	0.0015	44	0.128	302	13
Jun.	0.1036	0.0129	0.0011	0.0124	0.0014	36	0.125	293	7
Jul.	0.1017	0.0119	0.0016	0.0113	0.0011	32	0.117	275	9
Aug.	0.0934	0.0111	0.0013	0.0106	0.0016	31	0.119	271	6
Spt.	0.0863	0.0096	0.0015	0.0092	0.0018	44	0.111	263	8
Oct.	0.0758	0.0087	0.0019	0.0081	0.0015	45	0.115	251	13
Nov.	0.0646	0.0064	0.0013	0.0068	0.0012	49	0.099	274	15
Dec.	0.0538	0.0048	0.0011	0.0051	0.0014	43	0.089	263	11
Winter	0.0572	0.0057	0.0013	0.0055	0.0015	48	0.096	264	12
Spring	0.0869	0.0100	0.0016	0.0099	0.0014	45	0.115	300	13
Summer	0.0996	0.0119	0.0013	0.0114	0.0013	33	0.119	280	7
Autumn	0.0756	0.0082	0.0015	0.0080	0.0015	46	0.108	263	12

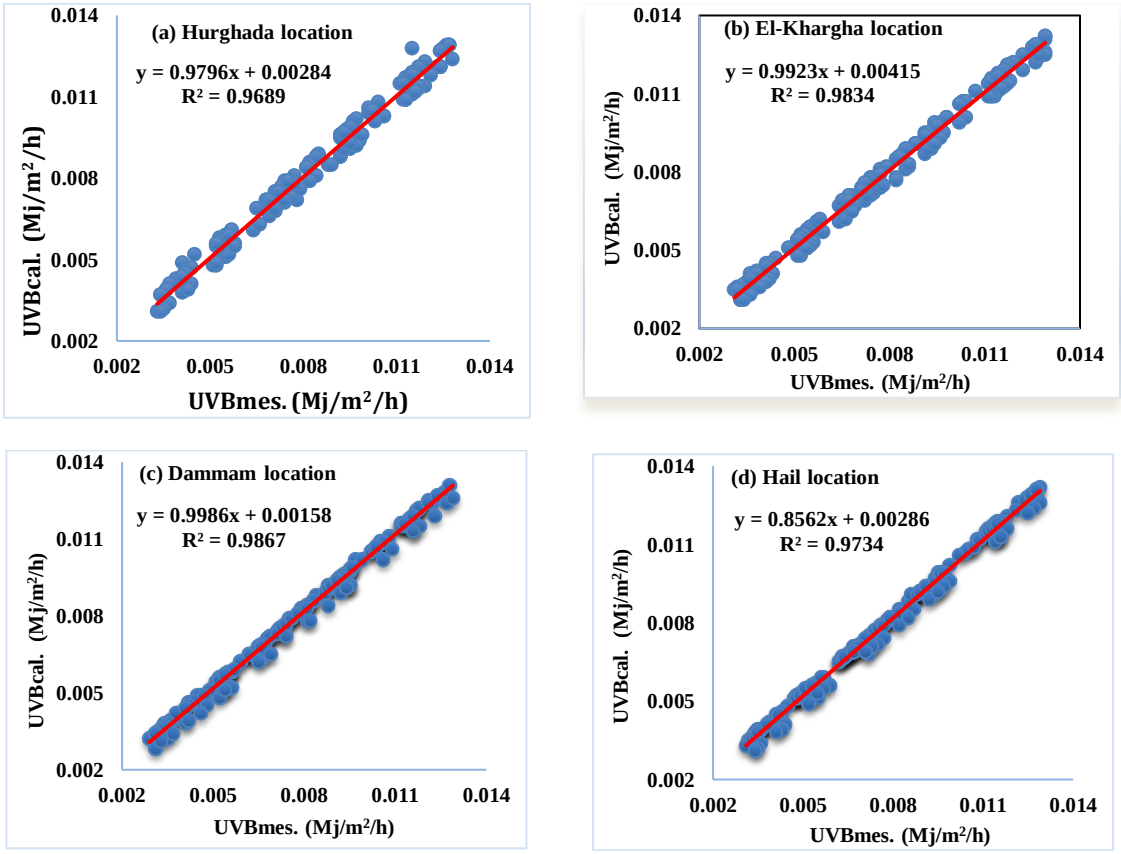

Fig. 2 The comparison between observed and calculated (UVB) solar radiation values for locations: (a) Hurghada, (b) El-Kharga, (c) Dammam (d) Hail in the present research.

The average hourly of UVB_{ext}. Solar energy ($MJ.m^{-2}h^{-1}$), and clearness index K_{tUVB} for Hurghada, El-Kharga, Dammam, and Hail locales from 1986 to 2020 are shown in Figure (3). According to this graph, the greatest average hourly $UVB_{ext.}$ solar energy values in the current research for the Hurghada, El-Kharga, Dammam, and Hail sites are 0.0937 ± 0.013, 0.0965 ± 0.015, 0.0928 ± 0.014, and 0.0919 ± 0.011 at 1200 LST, respectively. At the sites chosen for this study in Hurghada, El-Kharga, Dammam, and Hail, respectively, the values of $UVB_{ext.}$, solar energy are nearly 1.53 of the equivalent extraterrestrial global solar radiation (6.45 $MJ.m^{-2}h^{-1}$), (6.08 MJ. $m^{-2}h^{-1}$), (6.24 MJ. $m^{-2}h^{-1}$), and (5.99 MJ. $m^{-2}h^{-1}$). From 800 to 1600 LST, these ratios have virtually constant values for each hour. The average hourly UVBext. irradiance is reduced from 1200 to 1600 LST (0.0534 ± 0.011, 0.0578 ± 0.014, 0.0547 ± 0.013, 0.0523 ± 0.015) in the selected locations at Hurghada, El-Kharga, Dammam, and Hail, respectively. These values range from 1.37 to 1.78. Overall, according to this statistic, the estimated UVB solar radiation in the selected places is in reasonable agreement with the measured UVB solar radiation values, as was said before, UVBext. Behaviour is caused by the sun's evident daily movement around the Earth. Additionally, based on this figure, the values of (K_{tUVB}) are lower than the comparable kt values for global solar radiation; the relevant values for (K_{tUVB}) at 800, 1200, and 1600 LST at the Hurghada location are 0.091, 0.124, and 0.0654respectively. The values of (K_{tUVB}) in El-Kharga location are 0.097, 0.128 and 0.079 at 800, 1200 and 1600 respectively, in the same way the values of clearness index (K_{tUVB}) at 800, 1200 and 1600 LST in the locations Dammam and Hail are 0.084, 0.119, 0.068 and 0.088, 0.117, 0.065 respectively. The high, extremely constricted UVB sun radiation caused by stratospheric ozone and dissipating wonders caused the above results. The UVB transmission through the climate can be evaluated during the current investigation, where the typical hourly estimations of UVB transmission are declining due to the air as a daytime component.

Given that the air that the radiation must travel through has altered how much UVB reaches the Earth's surface, the highest and lowest estimates of UVB transmission occur individually at 1200 and 1600 LST. The length of the radiation's passage through the environment and the measurement of each attenuator along the way are both affected by this shift. As a result, the length at 1200 LST in the early afternoon is not as great as its attributes at 800 LST in the morning and 1700 LST in the evening.

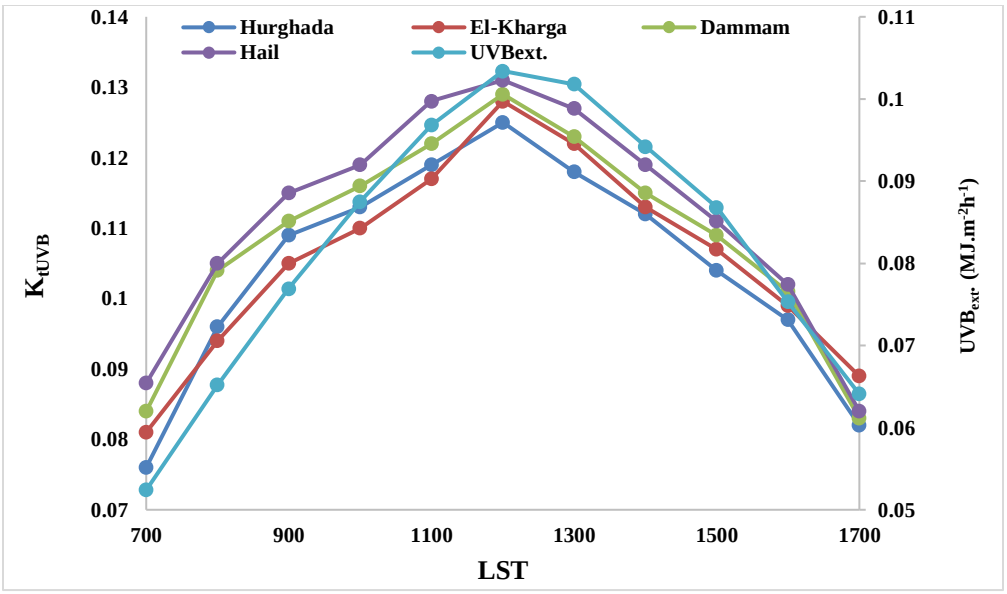

Fig. 3 Average hourly of UVBext., solar energy (MJ.m^{-2}h^{-1}), and clearness indices (K_{tUVB}) during the period time from 1986 to 2020 at selected locations in the present research.

Figure 4 displays the monthly average hourly percentage ratio (UVB/G %) for all sites chosen for the current study from 1986 to 2020. This graph shows that for all of the sites we chose, the largest percentage ratio values occur in the summer, while the least percentage ratio values occur in the winter. The change in the monthly average of hourly UVB/G% may be caused by the increase and decrease of the monthly average hourly values of both G and UVB, as seen from this figure. For all locations in the current study, the monthly average mean UVB/G varies from 0.15% (in January) to 0.30% (in June). However, for January and June, respectively, these figures indicate the arithmetic means of the average hourly UVB/G. The maximum values occur in June, maybe since June is the month when UVB and G radiation levels are at their highest on Earth in the Northern Hemisphere. The average hourly UVB/G% was also lower in the afternoon compared to the morning. For all sites included in this study, the difference between these values peaked in April (0.07%) and peaked in October (0.02%). The effect of aerosols on the fluctuation in air transparency may have contributed to the lower UVB/G% levels in the afternoon. The dust content in the atmosphere is due to the vertical mixing of particles developed because of increasing temperature. The results in this study are similar to those found in the previous study by [24, 27].

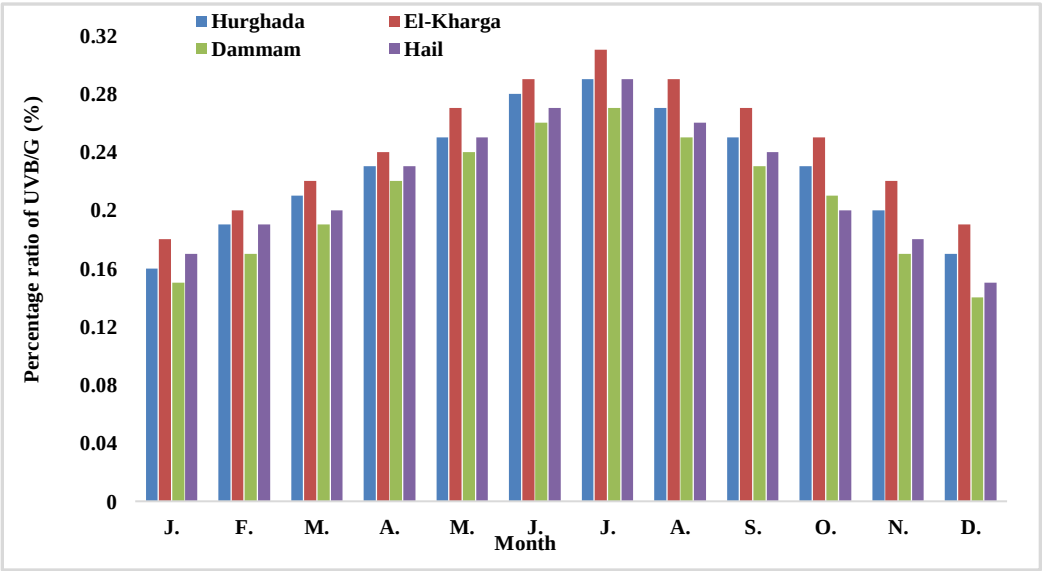

Fig. 4 The monthly hourly average (UVB/G %) from 1986 to 2020 in the present research.

The average hourly of UVB reduction (%) and UVB transmission (%) due to the atmosphere as a function of daytime during the period time from 1986 to 2020 for all locations in the present study are shown in figures (5-8). the average hourly UVB transmission (%) and reduction (%) due to the atmosphere as a function of daytime (0700-0800 to 1600-1700 LST). The highest and lowest values of UVB transmission occurring in (1100-1200 and 1600-1700 LST) were found at 13.26% and 2.61%, 16.41% and 3.58%, 16.55% and 3.15%, 16.35% and 3.55 for Hurghada, El-Kharga, Dammam and Hail locations respectively. This trend is expected given that the atmosphere through which the solar radiation must traverse has altered the UVB solar energy reaching the Earth's surface. The amount of each attenuator along the radiation's journey through the atmosphere and its length are also factors in this alteration. The path length is, however, shorter around midday (1100–1200 LST) than it is in the morning (0700–1000 LST) and afternoon (1500-1700 LST). Accordingly, for Hurghada, El-Kharga, Dammam, and Hail sites, respectively, the lowest and greatest values of UVB solar energy reduction from the atmosphere were 86.74% and 97.39%, 83.59% and 96.42, 83.45% and 96.85%, 83.65%, and 96.45%. It was discovered that the atmosphere might drastically lower UVB solar energy. For Hurghada, El-Kharga, Dammam, and Hail, respectively, the average UVB solar energy reduction values for this research were 92.21%, 90%, 90.2%, and 90.1. In contrast, the average air transmittance of UVB solar energy at Hurghada, El-Kharga, Dammam, and Hail is 7.79%, 10%, 9.8%, and 9.9, respectively. Additionally, for the locations of Hurghada, El-Kharga, Dammam, and Hail, respectively, the hourly average UVB solar energy reduction values for the time from 1500 to 1700 LST (96.5%, 95%, 95.2%, and 94.5) are higher than these values for the time from 0700 to 1000 LST (91%, 89.1%, 89.5%, and 89%). Additionally, the average UVB solar energy reduction values at noon (1100–1300 LST) were 89%, 85%, 86.3, and 86.5% for the Hurghada, El-Kharga, Dammam, and Hail, respectively. This investigation's results are similar to those obtained from other studies [22, 25]. These results may be caused by an increase in aerosols in the atmosphere throughout the afternoon (1500 to 1700 LST); we examined the atmospheric transparency for selected locations in the present research to determine the values of direct solar energy.

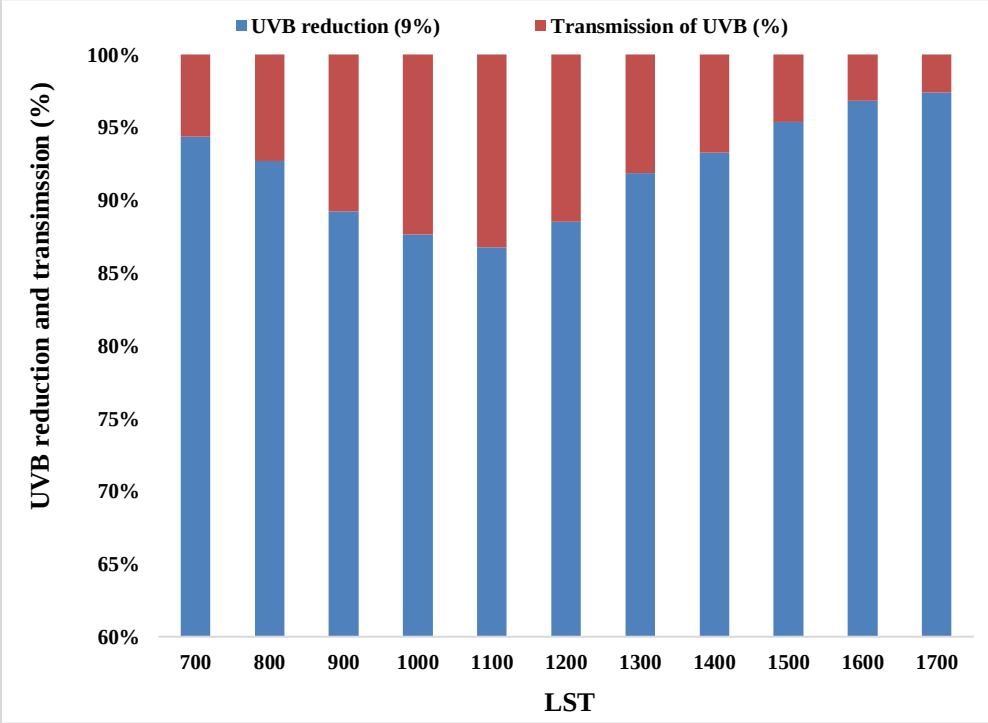

Fig. 5 The average hourly of UVB reduction (%) and UVB transmission (%) due to the atmosphere as a function of daytime during the period time from 1986 to 2020 at the Hurghada site.

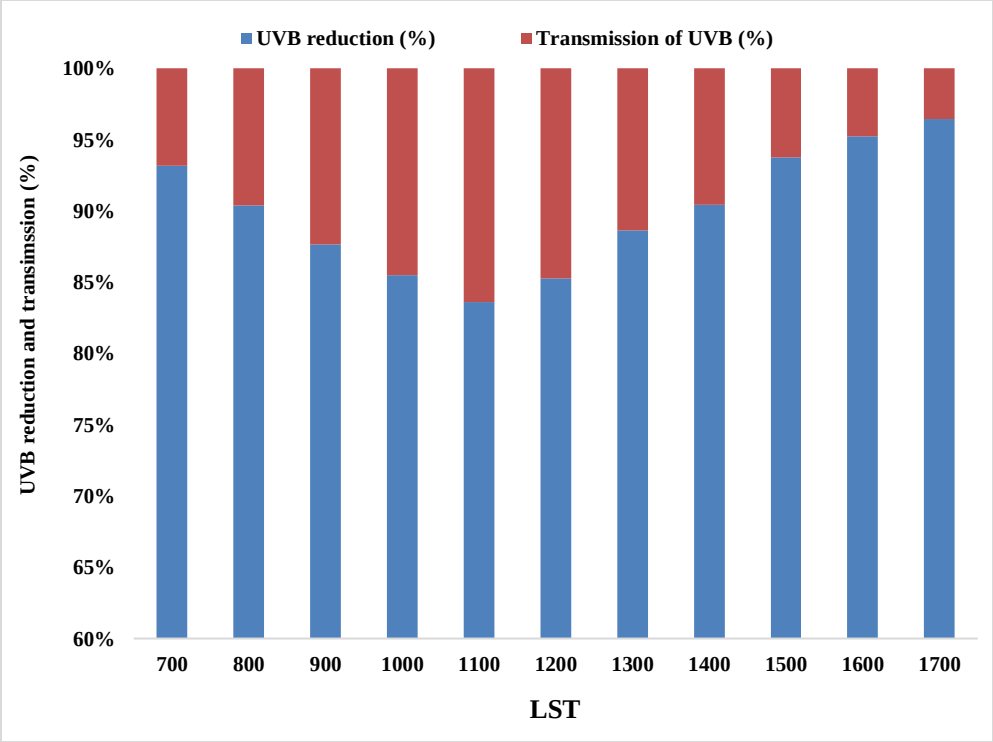

Fig. 6 The average hourly of UVB reduction (%) and UVB transmission (%) due to the atmosphere as a function of daytime during the period time from 1986 to 2020 at the El-Kharga site.

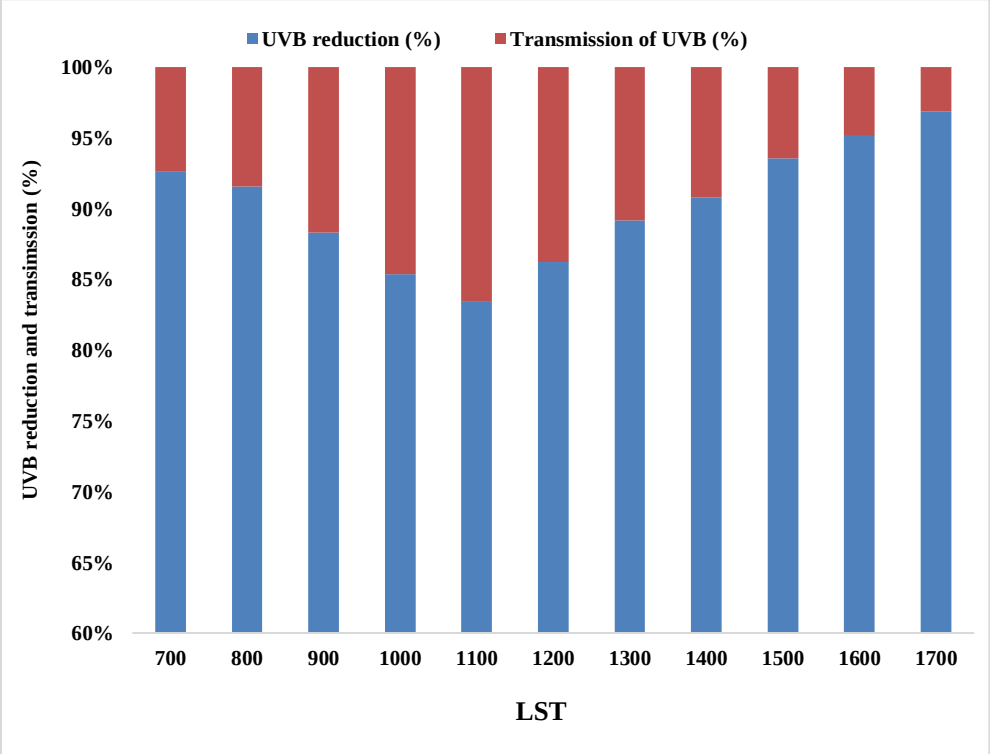

Fig. 7 The average hourly of UVB reduction (%) and UVB transmission (%) due to the atmosphere as a function of daytime during the period time from 1986 to 2020 at the Dammam site.

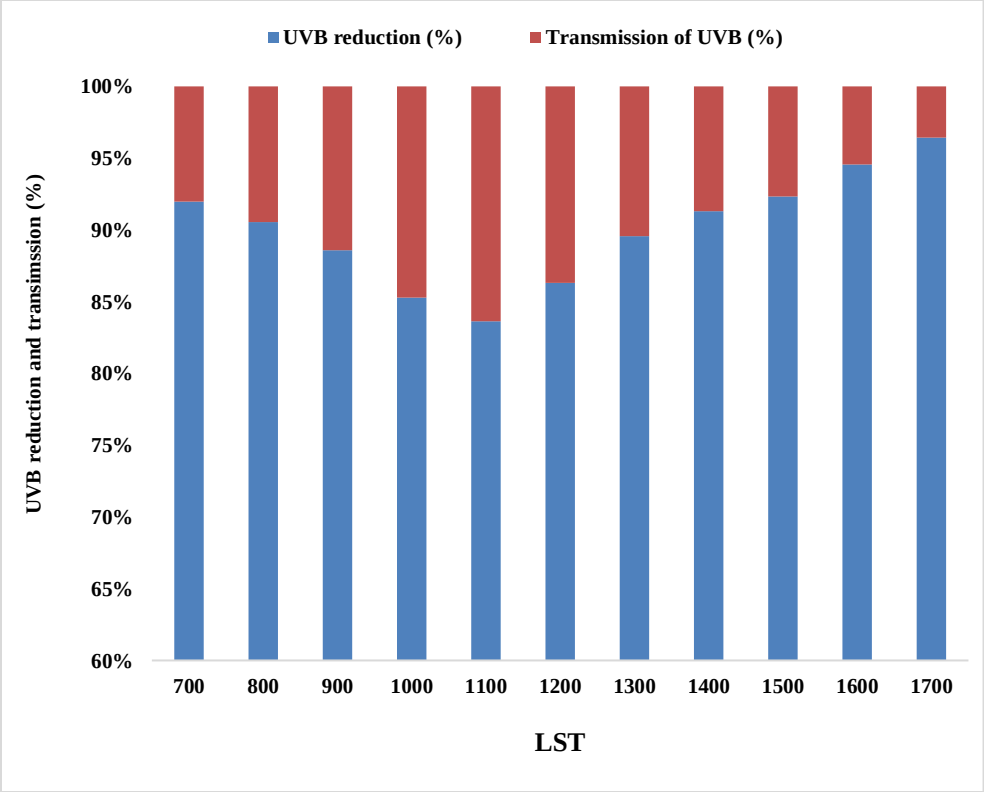

Fig. 8 The average hourly of UVB reduction (%) and UVB transmission (%) due to the atmosphere as a function of daytime during the period time from 1986 to 2020 at the Hail site.

The average monthly mean values of the UV index (UVI) solar radiation from 1986 to 2020 around noontime (10 am – 2 pm) at the selected sites in the present work are illustrated in figure 9. Looking at this graph, we can see that the highest UVI values at the study's chosen locations occur around the summer months. In contrast, the lowest UVI values occur around the winter months, with spring and autumn months falling somewhere in between. The high UVI levels are shown in this figure to range between 12.6, 13.4, 11.3, and 11.1 at the Hurghada, El-Kharga, Dammam, and Hail sites, respectively, while the low UVI levels in the sites chosen for the current study range between 4.1, 4.5, 3.7 and 3.4 at the Hurghada, El-Kharga, Dammam, and Hail locations, respectively. At Hurghada, El-Kharga, Dammam, and Hail, respectively, the discrepancies between high and low levels in the current study are between 32.5%%, 33.6%, 32.7%, and 30.1%. Therefore, El-Kharga and Dammam sites have the highest variance of levels, while Hail and Hurghada sites have the lowest variance. The lowest UVI values found in December and January at Hurghada, El-Kharga, Dammam, and Hail, respectively, were 4.2, 4.7, 3.8, and 3.5. However, high UVI levels of 12.2, 13, 11.7, and 10.7 were discovered in the months of June and July in Hurghada, El-Kharga, Dammam, and Hail, respectively. Additionally, the spring and autumnal months of Hurghada, El-Kharga, Dammam, and Hail were found to have moderate UVI values of 8.5, 8.9, 7.1, and 6.5, respectively. Figure 10 shows the agreement between measured and predicted (UVI) solar radiation values for the following places in the current study: (a) Hurghada, (b) El-Kharga, (c) Dammam, and (d) Hail. The observed and computed UVI values showed good agreement.

Figure (11), which depicts the average monthly association between the UVI and sun zenith angle (SZA) at the chosen locales from 1986 to 2020, is shown in Hurghada, El-Kharga, Dammam, and Hail. This chart shows an inverse relationship between UVI levels and the sun zenith angle (SZA) at all chosen locations. The data in this research were collected at midday because solar radiation travels the shortest distance through the atmosphere, minimizing the impact of atmospheric components. The solar zenith angle (SZA) is the cause of variations in UVI by 93%, 91%, 92%, and 91.5% at Hurghada, El-Kharga, Dammam, and Hail in the current research, as shown by this figure. Additionally, the monthly average has a correlation coefficient of 93%, 91%, 92%, and 91.5% at the Hurghada, El-Kharga, Dammam, and Hail sites, respectively.

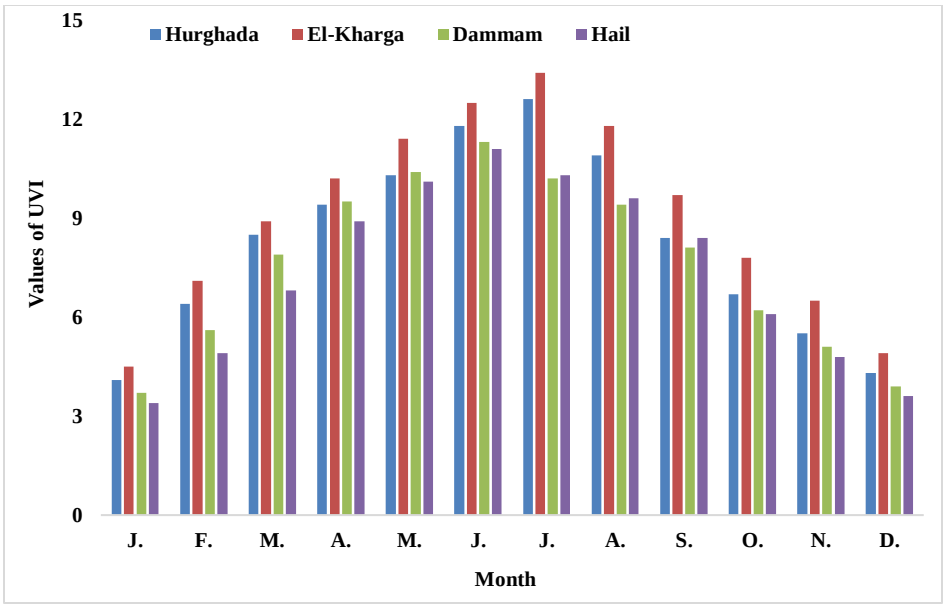

Fig. 9 The average monthly mean of the UV index (UVI) solar radiation from 1986 to 2020 around noontime (10 am – 2 pm) at the selected sites in the present work

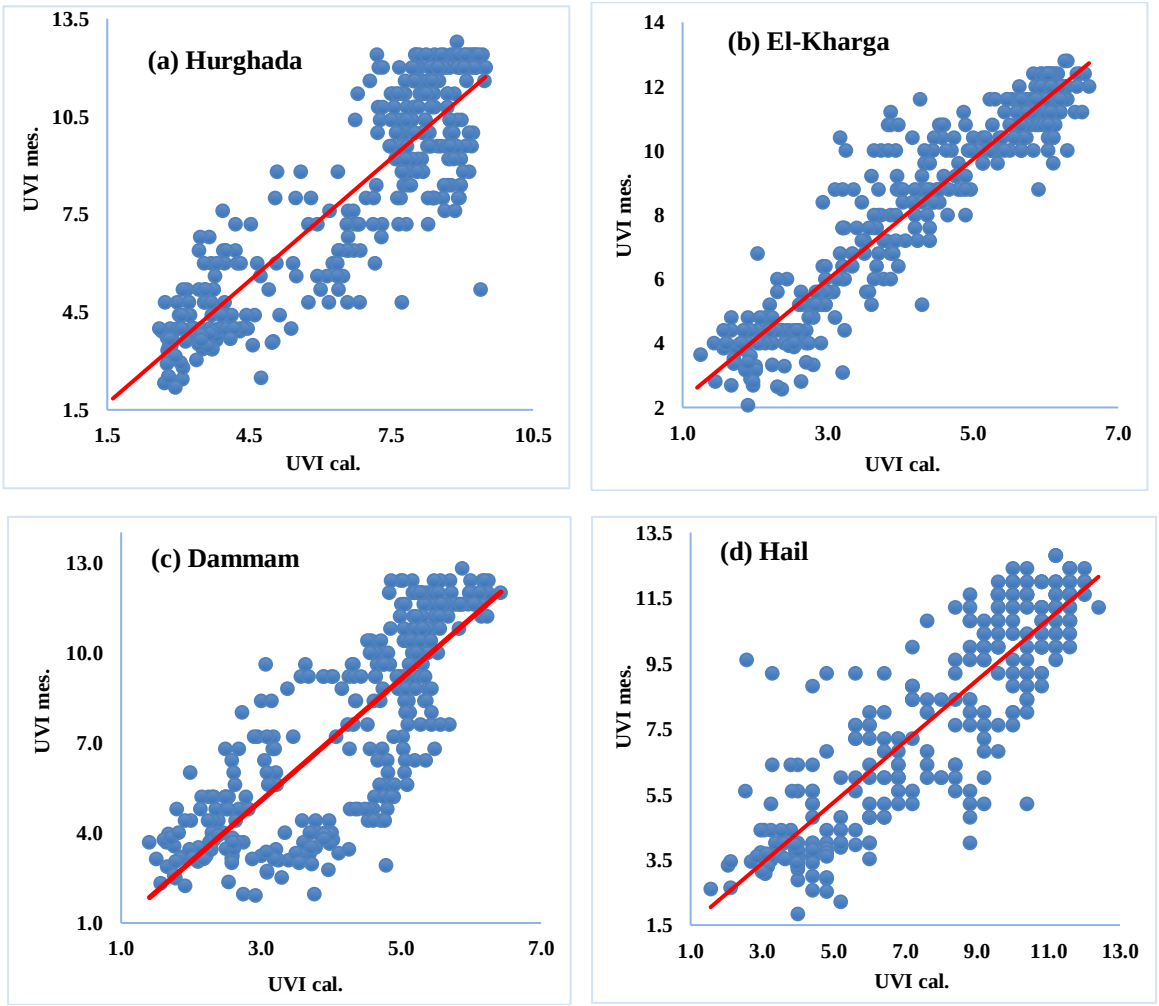

Fig. 10 The correlation between observed and calculated (UVI) solar radiation values for locations: (a) Hurghada, (b) El-Kharga, (c) Dammam (d) Hail in the present research.

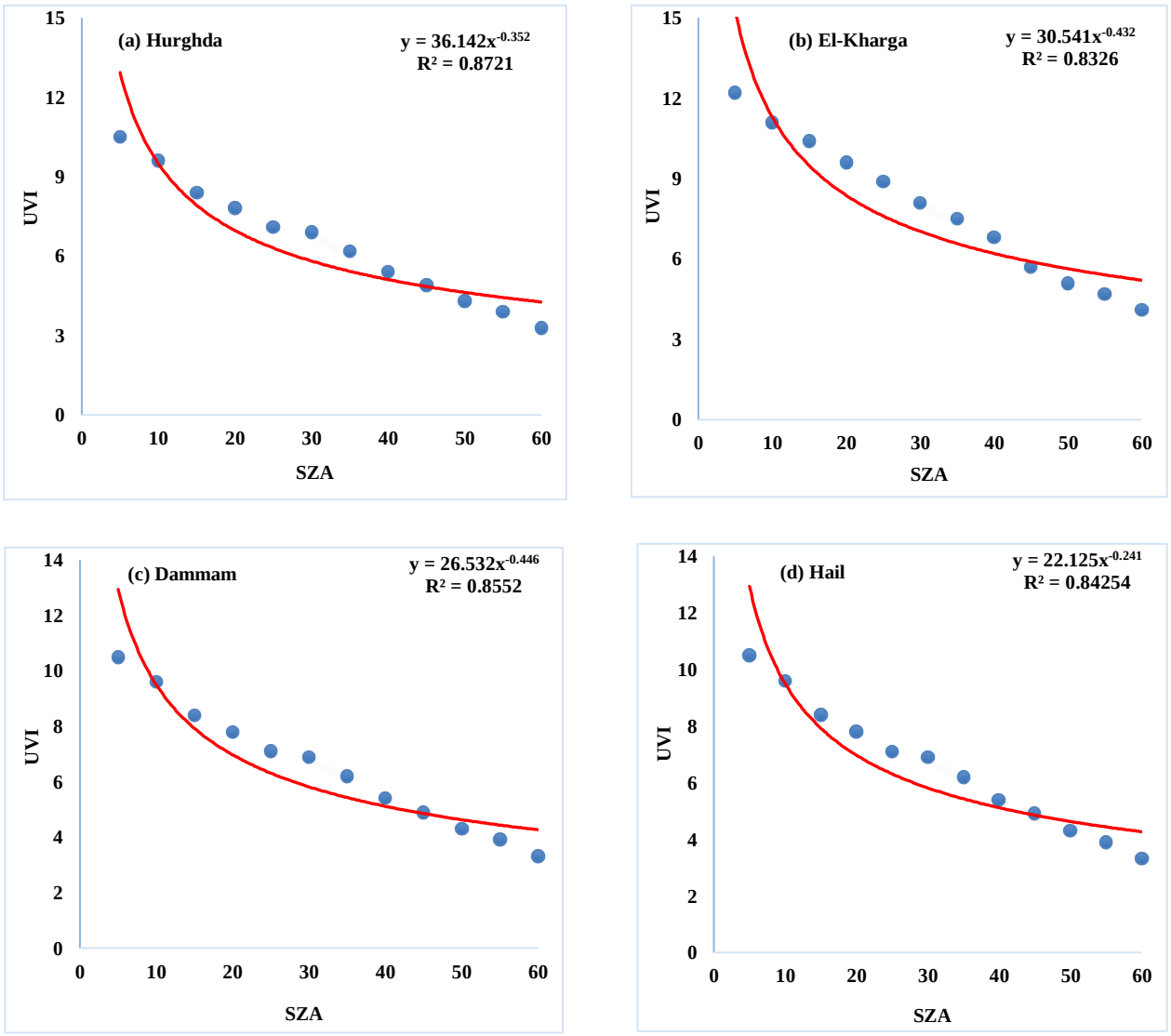

Fig. 11 The average monthly values of UVI and ZSA through 1986 - 2020 in the present research at selected locations; (a) Hurghada, (b) El-Kharga, (c) Dammam, (d) Hail.

In the current study at selected locations (Hurghada, El-Kharga, Dammam, and Hail), the power low function between monthly averages of UVB atmospheric transmission (K_{tUVB}) and slant ozone column (Z) for over the entire sky during the time from 1986 to 2020 is depicted in figures 12-15, respectively. The cloudiness condition was represented by the atmospheric transmission for solar total horizontal irradiance, often known as the clearness index (k_t). The fact that the cloudiness index and UVB measurements are being conducted simultaneously in this study is a significant benefit. Figures 12–15 demonstrate that linear regression analysis was conducted to assess the association between the monthly values of UVB transmission and slant ozone. Equations (13–16) in the current study provide the power law connection describing the dependency of UVB transmission on slant ozone for selected sites. For Hurghada, El-Kharga, Dammam, and Hail, this connection's correlation (R2) were 0.76, 0.72, 0.84, and 0.69, respectively. The fluctuation of other components, such as aerosols and tropospheric ozone, which were not considered in this study, should be blamed for the remaining variance.

$$K_{tUVB} = 52\ (Z)^{-1.058}\ (R^2 = 0.76) \text{ for Hurghada} \quad (13)$$

$$K_{tUVB} = 58\ (Z)^{-1.003}\ (R^2 = 0.72) \text{ for El-Kharga} \quad (14)$$

$$K_{tUVB} = 47\ (Z)^{-1.027}\ (R^2 = 0.84) \text{ for Dammam} \quad (15)$$

$$K_{tUVB} = 41\ (Z)^{-1.087}\ (R^2 = 0.69) \quad \text{for Hail} \quad (16)$$

The values of RAF for the monthly mean values under clear skies were equal to 1.058 for the Hurghada site in figure 12, 1.003 for the El-Kharga site in figure 13, 1.027 for the Dammam site in figure 14, and 1.087 for the Hail site in figure 15. These values were derived from Equations (13–16) and in comparison with Equation (12). Accordingly, the monthly mean values for clear sky circumstances for Hurghada, El-Kharga, Dammam, and Hail were 1.058%, 1.003%, 1.027%, and 1.087%, respectively, for the percentage increase in UVB that would occur from a 1% drop in the slant column ozone. These results show that, for the monthly mean values under clear skies, UVB values rise by 1.058%, 1.003%, 1.027%, and 1.087% if the slant ozone value at all examined sites decreases by 1%. Ozone variations at high angles clearly result in non-linear UVB transmission. The values of RAF in this study were comparable to those of the other authors [24, 25].

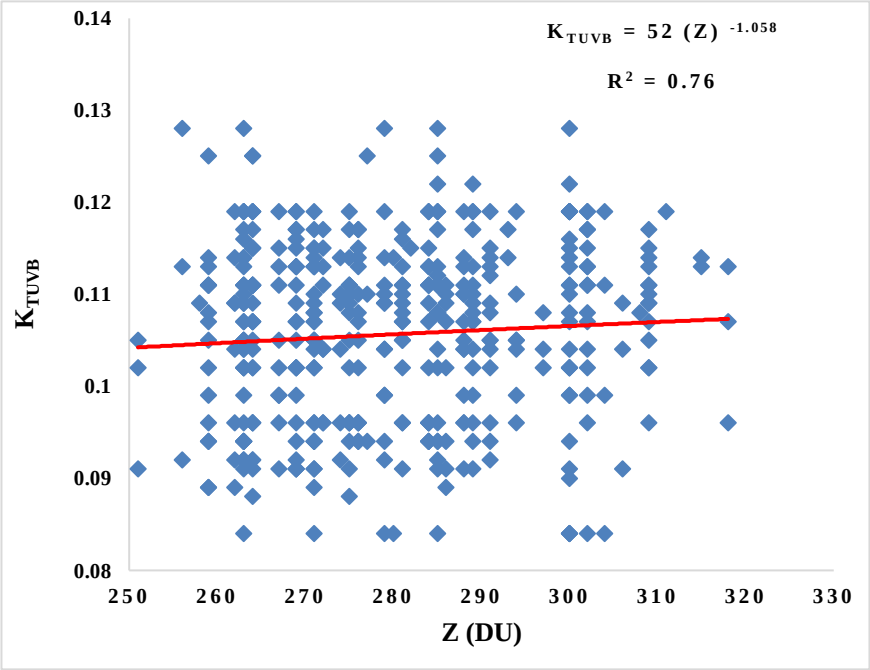

Fig. 12 The low power function between averages monthly of UVB atmospheric transmission (K_{tUVB}) and slant ozone column (z) for over the whole sky at the Hurghada site through the period from 1986 to 2020.

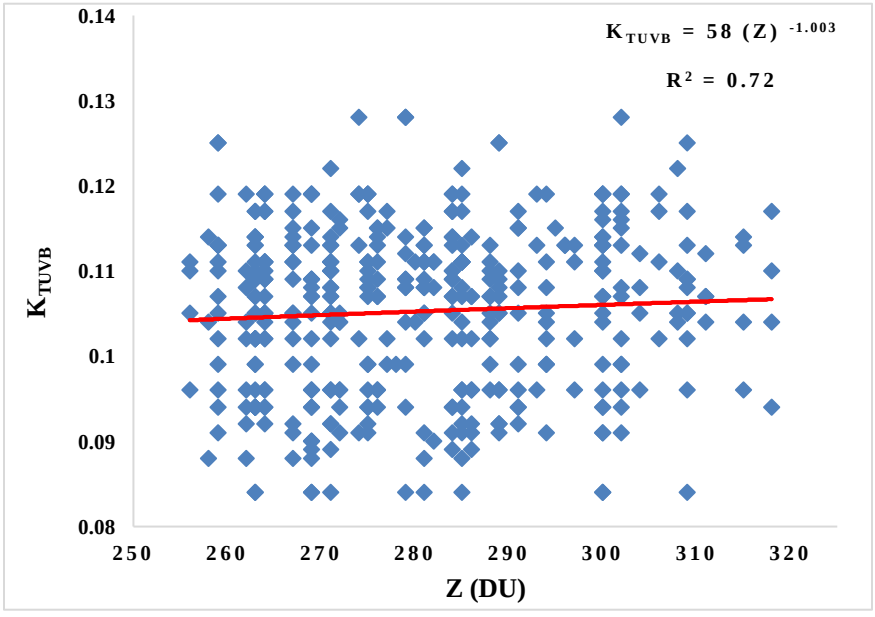

Fig. 13 The low power function between averages monthly of UVB atmospheric transmission (K_{tUVB}) and slant ozone column (z) for over the whole sky at the El-Kharga site through the period from 1986 to 2020.

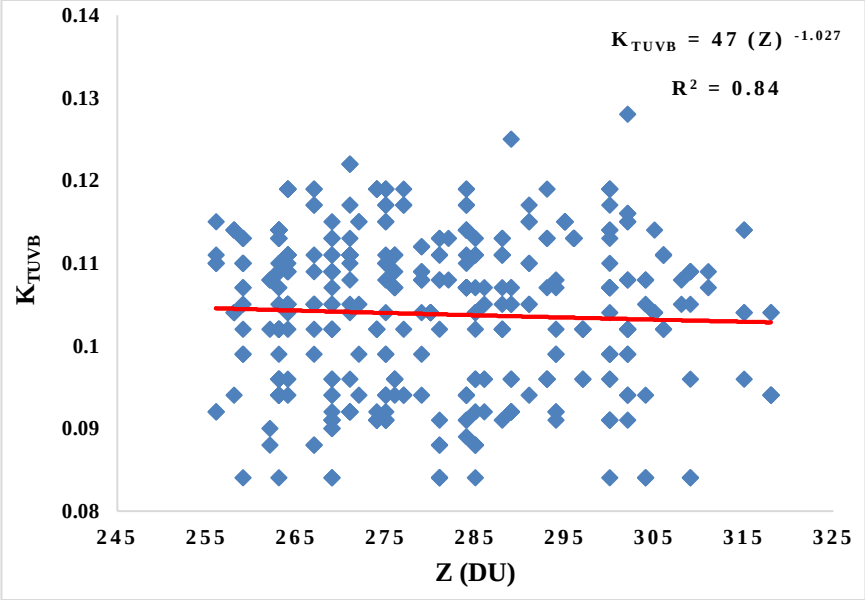

Fig. 14 The low power function between averages monthly of UVB atmospheric transmission (K_{tUVB}) and slant ozone column (z) for over the whole sky at the Dammam site through the period from 1986 to 2020.

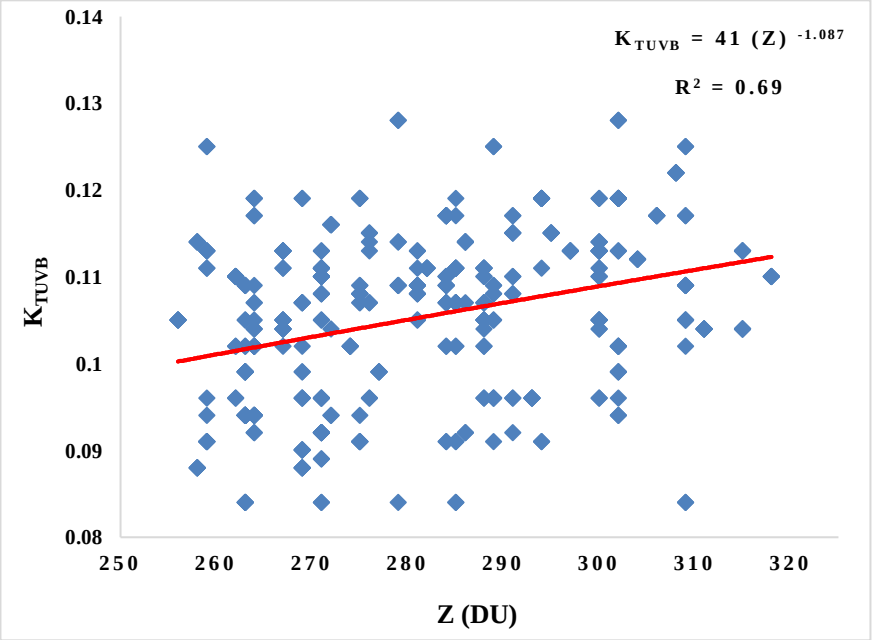

Fig. 15 The low power function between averages monthly of UVB atmospheric transmission (K_{tUVB}) and slant ozone column (z) for over the whole sky at the Hail site through the period from 1986 to 2020.

6. Conclusion

In the present research evaluated the effect of atmospheric transmittance of UVB Solar irradiance to broadband solar radiation in different climate sites during a period time from 1986 to 2020 for all weather conditions. The calculated values of UVB solar energy levels and the measured UVB solar radiation values coincide well. The discrepancy between measured and calculated UVB solar energy values ranges from 1% to 2.2%. The ratio of the average hourly UVB radiation intensities to the total global solar radiation in the current study from 1968 to 2020 was 0.294%, whereas the ratio of $UVB_{ext.}$ to the corresponding $G_{ext.}$, $UVB_{ext.}/G_{ext.}$, was 1.563%, demonstrates the much greater degree of attenuation of UVB relative to global solar radiation. The comparison between the observed and calculated data of UVB solar energy is in good agreement with them. The values of $UVB_{ext.}$, solar energy are nearly 1.53 of the equivalent extraterrestrial global solar radiation (6.45 $MJ.m^{-2}h^{-1}$), (6.08 MJ. $m^{-2}h^{-1}$), (6.24 MJ. $m^{-2}h^{-1}$), and

(5.99 MJ. $m^{-2}h^{-1}$). From 800 to 1600 LST, these ratios have virtually constant values for each hour. The highly extremely constricted UVB solar energy caused by stratospheric ozone and dissipating wonders caused the above results. The UVB transmission through the climate can be evaluated during the current investigation, where the typical hourly estimations of UVB transmission are declining due to the air as a daytime component.

The change in the monthly average of hourly UVB/G% may be caused by the increase and decrease of both G and UVB's monthly average hourly values. The monthly average mean UVB/G varies from 0.15% in January to 0.30% in June. The average hourly UVB/G% was also lower in the afternoon compared to the morning. The effect of aerosols on the fluctuation in air transparency may have contributed to the lower UVB/G% levels in the afternoon. The dust content in the atmosphere is due to the vertical mixing of particles developed because of increasing temperature. The highest and lowest values of UVB transmission occurring in (1100-1200 and 1600-1700 LST) were found at 13.26% and 2.61%, 16.41% and 3.58%, 16.55% and 3.15%, 16.35% and 3.55 for Hurghada, El-Kharga, Dammam and Hail locations respectively. This trend is expected given that the atmosphere through which the solar radiation must traverse has altered the UVB solar energy reaching the Earth's surface. The average UVB solar energy reduction values for this research were 92.21%, 90%, 90.2%, and 90.1. The UVB solar energy reduction values at noon (1100–1300 LST) were 89%, 85%, 86.3, and 86.5% for the sites in the present study.

The agreement between measured and predicted (UVI) solar radiation values for all sites in the present study is good. Inversely, the relationship between UVI levels and solar zenith angle (SZA) at all selected locations. The solar zenith angle (SZA) is the cause of variations in UVI by 93%, 91%, 92%, and 91.5% at Hurghada, El-Kharga, Dammam, and Hail, respectively, in the current research. The monthly mean values of RAF under clear skies were equal to 1.058, 1.003, 1.027, and 1.087 for Hurghada, El-Kharga, Dammam, and Hail sites in the present research. The percentage increase in UVB would occur from a 1% drop in the slant column ozone. These results show that, for the monthly mean values under clear skies, UVB values rise by 1.058%, 1.003%, 1.027%, and 1.087% if the slant ozone value at all examined sites decreases by 1%. Ozone variations at high angles clearly result in non-linear UVB transmission.

Nomenclature

UV	is the ultraviolet solar radiation (MJ m^{-2} h^{-1}) at wavelength (100-400nm).
UVB	is the ultraviolet solar radiation (MJ m^{-2} h^{-1}) at wavelength (280-315nm).
$UVB_{ext.}$	is the extraterrestrial solar radiation on the horizontal surface (MJ m^{-2} h^{-1}).
UVI	is the ultraviolet solar radiation index.
K_{tUVB}	is the clearness index.
TOC	is the total ozone column.
E_λ	is the ultraviolet spectrum wavelength dependent ($Wm^{-2}nm^{-1}$).
S_{er}	is the erythema weighting function accepted by CIE.
I_{SCUVB}	is the UVB solar constant (21.51 Wm^{-2}).
E_o	is the correction factor for the eccentricity of the Earth's orbit.
θ	is the solar elevation angle.
ω	is the solar angle.
SZA	is the solar zenith angle.
R	is the correlation coefficient.

References

[1] Basset AH, Korany HM, "Global and UVB Radiation Over Egypt," *Atmo´sfera*, vol. 20, pp. 341–358, 2007.

[2] Bilbao JD, Mateos D, de Miguel A, "Analysis and Cloudiness Influence on UV Total Irradiation," *International Journal of Climatology*, vol. 31, pp. 451–460, 2011.

[3] Samy A. Khalil, "Performance Evaluation and Statistical Analysis of Solar Energy Modeling: A Review and Case Study," *Journal of the Nigerian Society of Physical Sciences*, vol. 4, pp. 812, 2022.

[4] El-Metwally M, "Simple New Methods to Estimate Global Solar Radiation Based on Meteorological Data in Egypt," *Atmospheric Research*, vol. 69, pp. 217-239, 2004.

[5] Samy A. Khalil, Ashraf S. Khamees, Mostafa Morsy, A. H. Hassan, U. Ali Rahoma, Tarek Sayad, "Evaluation of Global Solar Radiation Estimated from ECMWF-ERA5 and Validation with Measured Data Over Egypt," *Turkish Journal of Computer and Mathematical Education*, vol. 12, no. 6, pp. 3996-4012, 2021.

[6] El Shazly SM, "A Study of Atmospheric Transparency Over Qena, Upper Egypt," *Water Air Soil Pollution,* vol. 94, pp. 259–273, 1997.

[7] El Shazly SM, Abdelmageed AM, Hassan GY, Noubi B, "Atmospheric Extinction Related to Aerosol Mass Concentration and Meteorological Conditions in the Atmosphere of Qena, Egypt," *Mausam*, vol. 42, pp. 367–374, 1991.

[8] El Shazly SM, Kassem KO, Hassan AA, El-Noubi EF, "An Empirical Model to Estimate UV Index in Some Upper Egypt Regions," *Resource Environment,* vol. 2, pp. 216–227, 2012. Doi: 10.5923/j.re.20120205.05.

[9] El-Noubi EF, "*Surface Ultraviolet Radiation Measurements in Qena, Egypt*," MSc Thesis, South Valley University, Qena, Egypt, 2006.

[10] El-Noubi EF, "*Distribution of UV Index in Some Upper Regions*," Ph.D. Thesis, South Valley University, Qena, Egypt, 2012.

[11] Anton M, Serrano CML, Garcia JA, "An Empirical Model to Estimate Ultraviolet Erythemal Transmissivity," *Annales Geophysicae,* vol. 27, pp. 1387–1398, 2009.

[12] Adam ME-N, "*Studies of Solar Radiation Components Related to Aerosols in the Atmosphere at Qena, Upper Egypt*," MSc Thesis, South Valley University, Qena, Egypt, 1995.

[13] Adam ME-N, "Effect of Stratospheric Ozone on UVB Solar Radiation Reaching the Earth's Surface at Qena, Egypt," *Atmospheric Pollution Research*, vol. 1, pp. 155–160, 2010.

[14] Adam ME-N, "Effect of Macrophysical Parameters of Clouds on Broadband Solar Radiation (295 – 2800 Nm) at a Subtropical Location," *Atmospheric and Oceanic Science Letters*, vol. 4, pp. 180–185, 2011b.

[15] Adam M E-N, "Uses Sunshine Duration to Estimate UVB Solar Radiation Under Sky Cover Conditions at Qena (Egypt)," *Canadian Journal on Computing in Mathematics, Natural Sciences, Engineering and Medicine*, vol. 3, pp. 7–24, 2012.

[16] Adam ME-N, "Sensitivity Analysis of Aerosols' Effect in UVB Transmission to Solar Zenith Angle at a Subtropical Location (Qena, Egypt)," *Atmospheric Environment,* vol. 71, pp. 311–318, 2013.

[17] Adam ME-N, El Shazly M, "Attenuation of UVB Radiation in the Atmosphere: Cloud Effects at Qena (Egypt)," *Atmospheric Environment*, vol. 41, pp. 4856–4864, 2007.

[18] Salas L.F.S, Rojas J.L.F, Filho AJP, Karam H.A, "Ultraviolet Solar Radiation in the Tropical Central Andes (12.0 ◦S)," *Photochemical and Photobiological Sciences*, vol. 16, pp. 954–971, 2017.

[19] Foyo-Moreno I, Vida J, Alados-Arboledas L, "Ground-Based Ultraviolet (290–385 Nm) and Broadband Solar Radiation Measurements in Southeastern Spain," *International Journal of Climatology*, vol. 18, pp. 1389–1400, 1998.

[20] Lucas R.M, Byrne S.N, Correale J, Ilschner S, Hart P.H, "Ultraviolet Radiation, Vitamin D and Multiple Sclerosis," *Neurodegenerative Disease Management*, vol. 5, pp. 413–424, 2015.

[21] Lindqvist PG, Epstein E, Nielsen K, Landin-Olsson M, Ingvar C, Olsson H, "Avoidance of Sun Exposure as a Risk Factor for Major Causes of Death: A Competing Risk Analysis of the Melanoma in Southern Sweden Cohort," *Journal of Internal Medicine*, vol. 280, pp. 375–387, 2016.

[22] Saiz-Lopez A, Lamarque J.F, Kinnison D.E, Tilmes S, Ordóñez C, Orlando J.J, Conley A.J, Plane JMC, Mahajan A.S, Santos G.S, et al., "Estimating the Climate Significance of Halogen-Driven Ozone Loss in the Tropical Marine Troposphere," *Atmospheric Chemistry and Physics*, vol. 12, pp. 3939–3949, 2012.

[23] Cadet J.M, Portafaix T, Bencherif H, Lamy K, Brogniez C, Auriol F, Metzger J.M, Boudreault L.E, Wright C.Y, "Inter-Comparison Campaign of Solar UVR Instruments under Clear Sky Conditions at Reunion Island (21◦ S, 55◦ E)," *International Journal of Environmental Research, Public Health,* vol. 17, pp. 2867, 2020.

[24] Neto J.V, dos Santos C.B, Torres É.M, Estrela C, Boxplot: A Graphical Resource for Analyzing and Interpreting Quantitative Data," *Dental Bras. Cent.*, vol. 26, pp. 1–6, 2017.
[Online]. Available: https://www.robrac.org.br/seer/index.php/ ROBRAC/article/view/1132/897 (accessed on 8 January 2022).

[25] Lamy K, Portafaix T, Brogniez C, Godin-Beekmann S, Bencherif H, Morel B, Pazmino A, Metzger J.M, Auriol F, Deroo C, et al., "Ultraviolet Radiation Modelling from Ground-Based and Satellite Measurements on Reunion Island, Southern Tropics," *Atmospheric Chemistry and Physics*, vol. 18, pp. 227–246, 2018.

[26] WRC (World Radiation Centre), "International Perheliometers Comparison (IPC VI)," October Working Report 188, Davos, Switzerland, 1985.

[27] Robaa, S.M., "On the Estimation of UV−B Radiation Over Egypt," *IDOJARAS, Quarterly Journal of the Hungarian Meteorological Service*, vol. 112, pp. 45−60, 2008.

[28] Serrano A, Anton M, Cancillo M.L, Garcia J.A, "Proposal of a New Erythemal UV Radiation Amplification Factor," *Atmospheric Chemistry and Physics Discussion*, vol. 8, pp. 1089−1111, 2008.

[29] Samy A. Khalil, U. Ali Rahoma, A. H. Hassan, Rashed M. Greeb, "Assessment of UVB Solar Radiation in Four Different Selected Climate Locations in Saudi Arabia," *NRIAG Journal of Astronomy and Geophysics*, vol. 10, no. 1, pp. 125-137, 2021.